Surface wave in a Maxwell liquid-saturated poroelastic layer

A. El Baroudi *, J.Y. Le Pommellec

Arts et Métiers ParisTech, 2 bd du Ronceray, 49035 Angers, France

A B S T R A C T

An analytical approach of the propagation and attenuation of Love waves in a viscoelastic liquid-saturated poroelastic layer has been considered in this paper. The equations of motion have been formu-lated separately for different media under suitable boundary conditions at the interface of viscoelastic liquid, poroelastic layer and elastic substrate. Following Biot's theory of poroelasticity, a new accurate and simple generalized dispersion equation has been established to design Love wave liquid sensors. The effect of liquid shear viscosity on the Love waves velocity has been studied. The influence of thickness and porosity of the waveguide layer has also been shown on the Love waves velocity and attenuation. The various investigations results can serve as benchmark solutions in design of liquid sensors and nonde-structive testing.

Keywords:
Love wave
Maxwell liquid
Poroelastic material

1. Introduction

Surface acoustic wave have been successfully applied in many fields including material characterization, seismology and nondestructive testing. More recently, surface acoustic wave based sensors for applications to liquids environments have been extensively investigated [1–12]. The surface acoustic wave sensor directly contacts the liquid to be tested to characterize its physical properties.

In surface acoustic wave devices, the acoustic wave travels at the surface of the propagating medium and its energy is confined within one wavelength of depth; it follows that the surface acoustic wave properties (velocity and attenuation) are highly affected by any physical changes that occur at the surface of the propagating medium, when the surface acoustic wave device interacts with an external environmental stimuli. In the presence of a liquid environment, the wave properties can be perturbed by the changes in the physical properties of the liquid contacting the sensor surface.

The design of liquid sensors requires the selection of several parameters, such as the acoustic wave polarizations and the wave-guiding medium (i.e. finite thickness, homogeneous or non-homogeneous). This paper proposes a novel generalized dispersion equation to design Love wave liquid sensors, and intends the attention of the researchers to viscoelasticity of liquids and poroelasticity of layer that strongly affect the Love wave behavior.

* Corresponding author.
E-mail address: adil.elbaroudi@ensam.eu (A. El Baroudi).

https://doi.org/10.1016/j.apacoust.2019.107076

2. Theoretical analysis

Love waves are a type of surface acoustic wave characterized by one shear horizontal particle mechanical displacement component u_2 dominant over the vertical and longitudinal ones. The Love wave liquid sensor consists of piezoelectric substrate, guiding layer and sensitive liquid. Due to the in-plane polarization, the Love waves are suitable for travel at a surface contacting a liquid environment. The number of Love modes that can propagate in the layer/substrate medium depends on the layer thickness, but the essential condition for the propagation of the Love waves is that the shear bulk wave velocity of the substrate is larger than the shear bulk wave velocity of the layer. Higher order Love modes develop at their respective cut-off frequencies, which are related to the thickness of the layer: they are dispersive as their velocity depends on the layer thickness, rather than on the substrate and the layer's material properties. Therefore, to describe the waveguide structure that guides Love waves, we consider a three-layer system consisting of a viscoelastic liquid, a poroelastic layer and an elastic substrate, see Fig. 1. The finite substrate occupies the positive space $x_3 > 0$. The layer rests on top of the substrate and has thickness h. On top of that rests the viscoelastic liquid which occupies the negative half-space $x_3 < -h$.

2.1. Guiding poroelastic layer and elastic substrate

To get a solution for Love wave propagating in the poroelastic layer, Biot's theory is used [13,14]. The poroelastic layer is composed of a solid skeleton and pore space. Moreover, the Love wave

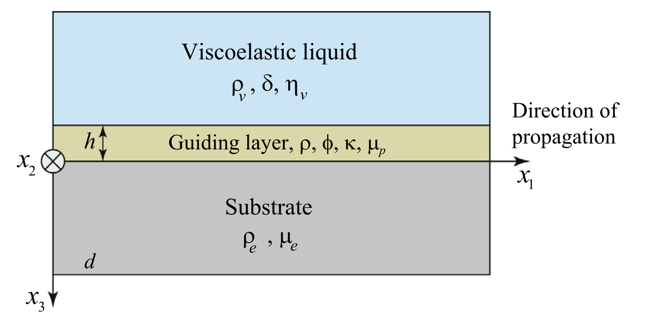

Fig. 1. The schematic representation of the Love wave. x_1: propagation direction of Love wave. x_2: polarization direction of Love wave. ρ_v, δ and η_v describe, respectively, the density, relaxation time and dynamic viscosity of the viscoelastic liquid. For the guiding poroelastic layer, ρ is the mixture density and the layer porosity and permeability are represented respectively by ϕ and κ; μ_p is the shear modulus of the porous framework. ρ_e and μ_e correspond to the density and shear modulus of the elastic substrate.

is taken to propagate in the x_1-direction, with shear displacement in the x_2-direction. A plane wave in the x_1-direction is considered, with displacement in x_2-direction only, $\mathbf{u}^{(p)} = \left(0, u_2^{(p)}, 0\right)$. Owing to symmetry, the displacement should be independent of $x_2, u_2^{(p)} = u_2^{(p)}(x_1, x_3)$. Therefore, the equation that governs the particle motion in a guiding layer saturated with a liquid is given by [15]

$$\left(b + m\frac{\partial}{\partial t}\right)\left(\frac{\partial^2}{\partial x_1^2} + \frac{\partial^2}{\partial x_3^2}\right)u_2^{(p)} - \frac{\rho}{\mu_p}\left[b + \left(m - \frac{\rho_f^2}{\rho}\right)\frac{\partial}{\partial t}\right]\frac{\partial^2 u_2^{(p)}}{\partial t^2} = 0 \tag{1}$$

where $b = \eta_f/\kappa$ and $m = \rho_f \tau/\phi$ represent respectively, the viscous and inertial coupling between the solid and fluid phases of the poroelastic layer [13]. Thus, the layer porosity and permeability are represented respectively by ϕ and κ; η_f describes the dynamic viscosity of the fluid phase and τ is the pores tortuosity. The parameter $\rho = \phi\rho_f + (1-\phi)\rho_s$ is the mixture density whereas ρ_f and ρ_s denote the densities of the solid and fluid phases of the poroelastic layer. In addition, μ_p is the shear modulus of the porous framework. Thus, in this work the substrate is considered to be a finite medium and the particle displacement $u_2^{(e)}$ is governed, using the elastodynamic theory by the Navier's equation

$$\left(\frac{\partial^2}{\partial x_1^2} + \frac{\partial^2}{\partial x_3^2}\right)u_2^{(e)} - \frac{1}{c_e^2}\frac{\partial^2 u_2^{(e)}}{\partial t^2} = 0 \tag{2}$$

where $c_e = \sqrt{\mu_e/\rho_e}$ is the bulk shear wave velocity in the substrate.

2.2. Viscoelastic liquid

To describe the viscoelasticity of the liquid, the Maxwell model which introduces a viscoelastic response of liquids at high frequencies is employed. The model consists of a spring and a damper connected in series. The damper represents energy losses and is characterized by the viscosity η_v, whereas the spring represents the energy storage and is characterized by the elastic shear modulus μ. These two quantities are related through the relaxation time δ, which is the characteristic time for the transition between viscous and elastic behavior $\delta = \eta_v/\mu$ (see for example [16]). Thus, the liquid motion is only produced by wave propagation in the poroelastic layer. Furthermore, since only shear deformation arises during transverse waves propagation, we can also ignore the pressure gradient. In addition, the linearized Navier-Stokes equation that governs the viscoelastic liquid motion can be simplified to the following

$$\left(\frac{\partial^2}{\partial x_1^2} + \frac{\partial^2}{\partial x_3^2}\right)v_2 - \frac{\rho_v}{\eta_v}\left(1 + \delta\frac{\partial}{\partial t}\right)\frac{\partial v_2}{\partial t} = 0 \tag{3}$$

where v_2 is the velocity component along the x_2-direction and ρ_v is the liquid density.

2.3. General solution of wave equations

For a plane harmonic wave propagation, the solution of Eqs. (1)–(3) are sought in the form

$$\left\{\begin{array}{c} v_2 \\ u_2^{(p)} \\ u_2^{(e)} \end{array}\right\}(x_1, x_3) = \left\{\begin{array}{c} V_2(x_3) \\ U_2^{(p)}(x_3) \\ U_2^{(e)}(x_3) \end{array}\right\} e^{j(kx_1 - \omega t)} \tag{4}$$

where ω is the angular frequency. Love wave propagating in the poroelastic layer undergoes attenuation, hence, the wavenumber k along the propagation direction of the Love wave becomes complex, $k = k_0 + j\alpha$, the real part k_0 describes the Love wave velocity, the imaginary part α, is the Love wave attenuation induced by the viscoelastic liquid. After substitution of Eq. (4) into Eqs. (1)–(3), the x_3 dependence can be expressed as

$$U_2^{(p)}(x_3) = A_p \cos\left(\beta_p x_3\right) + B_p \sin\left(\beta_p x_3\right),$$
$$U_2^{(e)}(x_3) = A_e e^{-\beta_e x_3} + B_e e^{\beta_e x_3}, \ V_2(x_3) = A_v e^{\beta_v x_3}$$

where A_p, B_p, A_e, B_e and A_v are arbitrary amplitudes and the wavenumbers β_p, β_e and β_v are given in the following form

$$\beta_p = \sqrt{\frac{\omega^2}{\mu_p}\left(\rho - \frac{\rho_f^2}{m + \frac{jb}{\omega}}\right) - k^2}, \ \beta_e = \sqrt{k^2 - \frac{\omega^2}{c_e^2}},$$
$$\beta_v = \sqrt{k^2 - \frac{j\omega\rho_v}{\eta_v}(1 - j\omega\delta)}$$

In addition, the shear stress components that will be used in boundary and interface conditions are given by

$$\left\{\begin{array}{c} \sigma_{23} \\ \sigma_{23}^{(p)} \\ \sigma_{23}^{(e)} \end{array}\right\} = \left\{\begin{array}{c} \frac{\eta_v}{1-j\omega\delta}\partial_{x_3} v_2 \\ \mu_p \partial_{x_3} u_2^{(p)} \\ \mu_e \partial_{x_3} u_2^{(e)} \end{array}\right\} = \left\{\begin{array}{c} \frac{\eta_v}{1-j\omega\delta}\Sigma_v(x_3) \\ \mu_p \Sigma_p(x_3) \\ \mu_e \Sigma_e(x_3) \end{array}\right\} e^{j(kx_1 - \omega t)} \tag{5}$$

where the x_3 dependence is defined as

$$\Sigma_p(x_3) = \beta_p\left[B_p \cos\left(\beta_p x_3\right) - A_p \sin\left(\beta_p x_3\right)\right],$$
$$\Sigma_e(x_3) = \beta_e\left(B_e e^{\beta_e x_3} - A_e e^{-\beta_e x_3}\right), \ \Sigma_v(x_3) = A_v \beta_v e^{\beta_v x_3}$$

2.4. Boundary conditions and dispersion relation

The following boundary conditions: continuity of shear stress and velocity (or displacement), and traction-free outer surface are suitable

$$v_2 + j\omega u_2^{(p)}|_{y=-h} = 0, \ \sigma_{23}^{(v)} - \sigma_{23}^{(p)}|_{y=-h} = 0,$$
$$u_2^{(p)} - u_2^{(e)}|_{x_3=0} = 0, \ \sigma_{23}^{(p)} - \sigma_{23}^{(e)}|_{x_3=0} = 0, \ \sigma_{23}^{(e)}|_{x_3=d} = 0$$

According to the above boundary conditions, the resolution of Eqs. (1)–(3) leads to the following equation:

$$\left[\mu_p^2\beta_p^2 + \frac{j\omega\eta_v\beta_v}{1 - j\omega\delta}\mu_e\beta_e \tanh\left(\beta_e d\right)\right]\sin\left(\beta_p h\right)$$
$$+ \mu_p\beta_p\left[\frac{j\omega\eta_v\beta_v}{1 - j\omega\delta} - \mu_e\beta_e \tanh\left(\beta_e d\right)\right]\cos\left(\beta_p h\right) = 0 \tag{6}$$

Eq. (6) represents the implicit dispersion equation of Love waves propagating in viscoelastic liquid-saturated poroelastic layer. To solve the Eq. (6) Mathematica Software is used to find the real and imaginary part of the wavenumber k. Thus, the Love wave velocity can be calculated as $v = \omega/k_0$ whereas the imaginary part describes the attenuation in the propagation direction. Furthermore, the critical term $\omega\delta$ in the Eq. (6) depends both on δ and ω. The three following regimes may be highlighted: (i) For $\omega\delta \ll 1$ the oscillation time ($= 1/\omega$) is greater than the relaxation time and, the liquid exhibits purely Newtonian behavior. (ii) For $\omega\delta \gg 1$ the oscillation time is smaller than the relaxation time and, the liquid exhibits viscoelastic behavior. (iii) At $\omega\delta = 1$ the transition from Newtonian to Maxwell regime takes place. Note that in the case of semi-infinite substrate, the dispersion Eq. (6) takes the following simplified form

$$\left(\mu_p^2\beta_p^2 + \frac{j\omega\eta_v\beta_v}{1 - j\omega\delta}\mu_e\beta_e\right)\sin(\beta_p h) + \mu_p\beta_p\left(\frac{j\omega\eta_v\beta_v}{1 - j\omega\delta} - \mu_e\beta_e\right)\cos(\beta_p h) = 0 \tag{7}$$

3. Results and discussion

The material properties given in Table 1 for the waveguide and substrate [15,12], and in Table 2 for viscoelastic liquid [12], are taken to construct this numerical example. In this work, numerical calculation is performed in the glycerol concentrations range from 15.4% to 88.0%.

The difference between the mechanical properties of the guiding layer and the substrate creates an entrapment of the acoustic energy in the guiding layer keeping the wave energy near the surface. This phenomenon makes Love wave devices very sensitive towards any changes occurring on the surface sensors. The Love waves exhibit a multimode character which depends on the layer thickness. As an example, Figs. 2(a) and 2(b) show the dispersion curves of Love wave velocity and attenuation of the first four modes. The Fig. 2(a) also shows the bulk shear wave velocity in the substrate and layer. When the guiding layer is very thin, the velocity of the first mode tends to the substrate bulk shear wave velocity; with increasing the layer thickness, the velocity of both the first and higher order modes asymptotically reaches the layer bulk shear wave velocity. Fig. 2(b) shows the Love wave attenuation of the first four modes with respect to the layer thickness. As can be seen, the attenuation increases with increasing the layer thickness and reaches a peak after which, with increasing the guiding layer thickness, it decreases. The peak of the attenuation decreases with increasing the mode order and the highest value corresponds to the fundamental mode. In addition, Fig. 3 shows the attenuation dispersion curves for the fundamental Love mode in poroelastic layer for different glycerol mass fraction. The attenuation increases with increasing the glycerol mass fraction and reaches the highest values for $h = 4.25$ µm.

Table 1
Material parameters.

Properties	Guiding layer and Substrate
μ_p (Pa)	3.91×10^{10}
η_f (mPa · s)	η_v
ρ_f (kg/m^3)	ρ_v
ρ_s (kg/m^3)	8900
κ (m^2)	10^{-18}
τ	3
μ_e (Pa)	5.8×10^{10}
ρ_e (kg/m^3)	2600
c_e (m/s)	4723.10

Table 2
Water-glycerol mixtures parameters. χ is the concentration of glycerol in water.

χ (%)	ρ_v (kg/m^3)	η_v (mPa · s)	δ (ps)
15.4	1017	1.4	28
32.9	1038	2.7	54
42.3	1050	3.8	76
52.2	1062	5.9	118
62.1	1075	10.2	204
72.0	1087	21.9	438
75.9	1093	33.2	664
80.0	1098	49.5	990
84.0	1104	81.8	1636
88.0	1109	128.1	2562

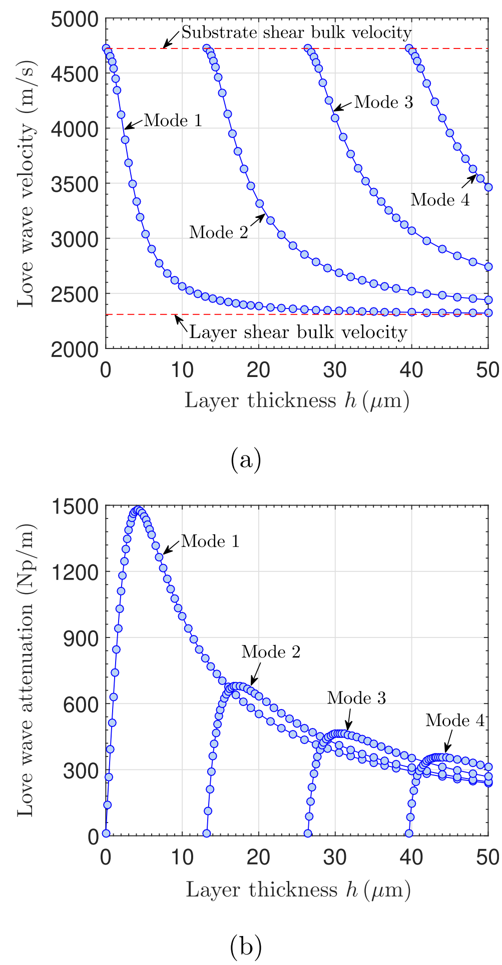

Fig. 2. Velocity and attenuation versus poroelastic layer thickness ($\phi = 0.2$) with $f = 100$ MHz and $\chi = 88\%$.

The influence of three layer porosities on the velocity and attenuation of the Love waves that propagate in the poroelastic layer saturated with a viscoelastic liquid is shown in Fig. 4 for the glycerol mass fraction of 88%. The velocity decreases as the layer thickness increases. Thus, the velocity for $\phi = 0.4$ are obviously larger than that for $\phi = 0.001$ and $\phi = 0.2$. However, Fig. 4 also illustrates that the attenuation increases with increasing the layer thickness and reaches a peak after which, with increasing the guiding layer thickness, it decreases. The peak of the attenuation decreases with increasing the layer porosity and the highest value corresponds to the smallest value of the layer porosity.

The dispersion curves of the Love wave velocity and attenuation versus frequency were also calculated and plotted as shown in

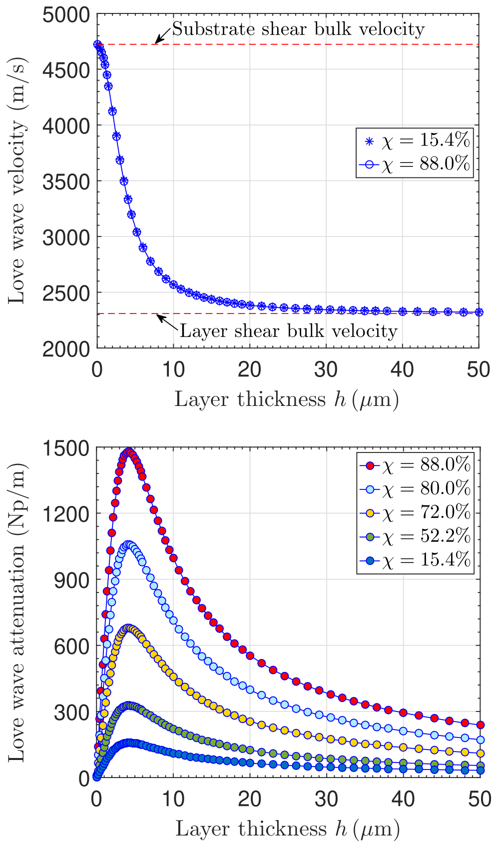

Fig. 3. Velocity and attenuation for the first mode versus poroelastic layer thickness ($\phi = 0.2$) with $f = 100$ MHz.

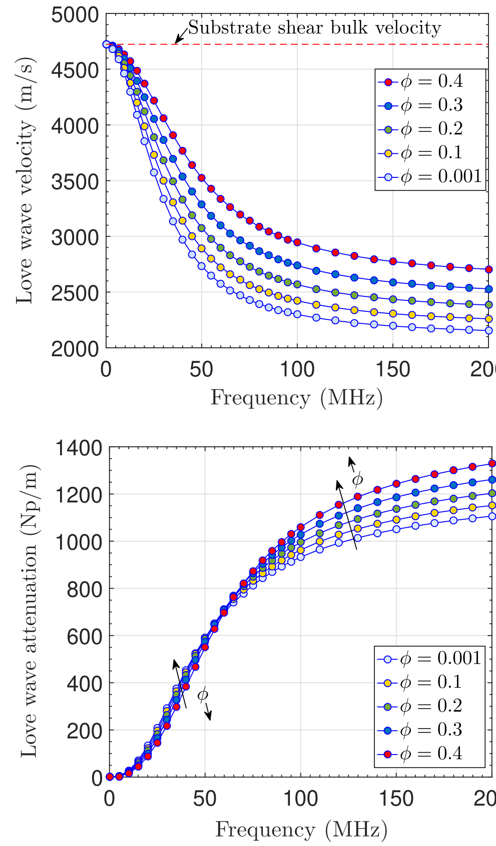

Fig. 5. Velocity and attenuation for the first mode versus frequency with $h = 10$ μm and $\chi = 88.0\%$.

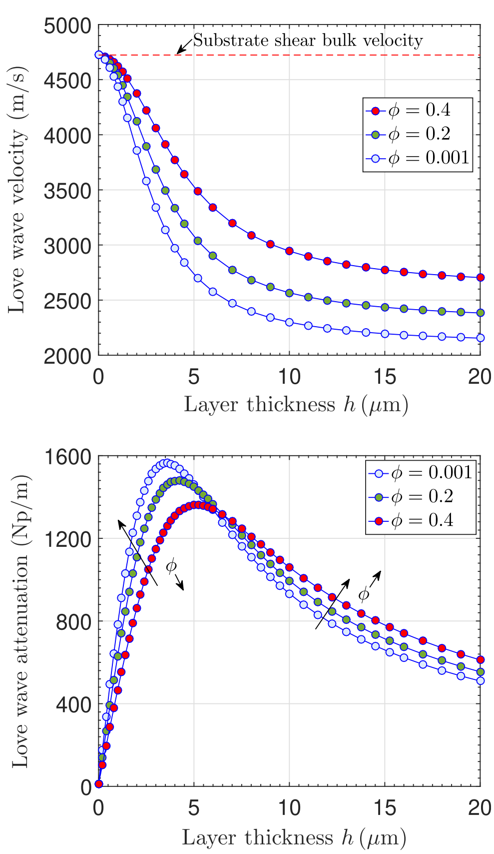

Fig. 4. Velocity and attenuation for the first mode versus poroelastic layer thickness with $f = 100$ MHz and $\chi = 88\%$.

Fig. 5. This Figure also illustrates the layer porosity effect on the dispersion curves of velocity and attenuation for different layer porosities (from 0.001 to 0.4). Fig. 5 shows that the velocity and attenuation are a monotonic function of the frequency. Fig. 5 indicates that the velocity increases with the increase of layer porosity. However, the attenuation increases with a decrease in the layer porosity when the layer thickness is lower than that of the peak given in the Fig. 4, and increases with an increase in the layer porosity when the layer thickness is higher than that of the peak.

The Love wave velocity variations in function of the glycerol mass fraction in both viscoelastic and Newtonian liquids are investigated in Fig. 6. Note that by considering a viscous liquid and increasing the shear viscosity, the Newtonian liquid model predicted a monotonically decreasing behavior between the velocity and the liquid shear viscosity. However, a Maxwell liquid model highlighted a non-monotonically decreasing relationship between the velocity and glycerol mass fraction. Therefore we can conclude that the non-monotonic behavior manifested the intrinsic viscoelastic properties of liquid [12]. Thus, Fig. 6 shows the velocity variation for different values of layer thickness and porosity. The elastic effects are significant for a glycerol concentration greater than 52.2%. For glycerol concentration values less than the critical value (52.2%), the liquid exhibits purely Newtonian behavior. The velocity dispersion between Newtonian and Maxwell behaviors becomes less remarkable as the layer thickness and porosity decreases.

The substrate thickness effect on Love wave velocity and attenuation has been examined by comparing the velocity and attenuation (v_f, α_f) when finite substrate is considered to the velocity and attenuation (v_{sf}, α_{sf}) when the substrate is assumed to be semi-infinite. Fig. 7 illustrates that the normalized velocity (v_f/v_{sf})

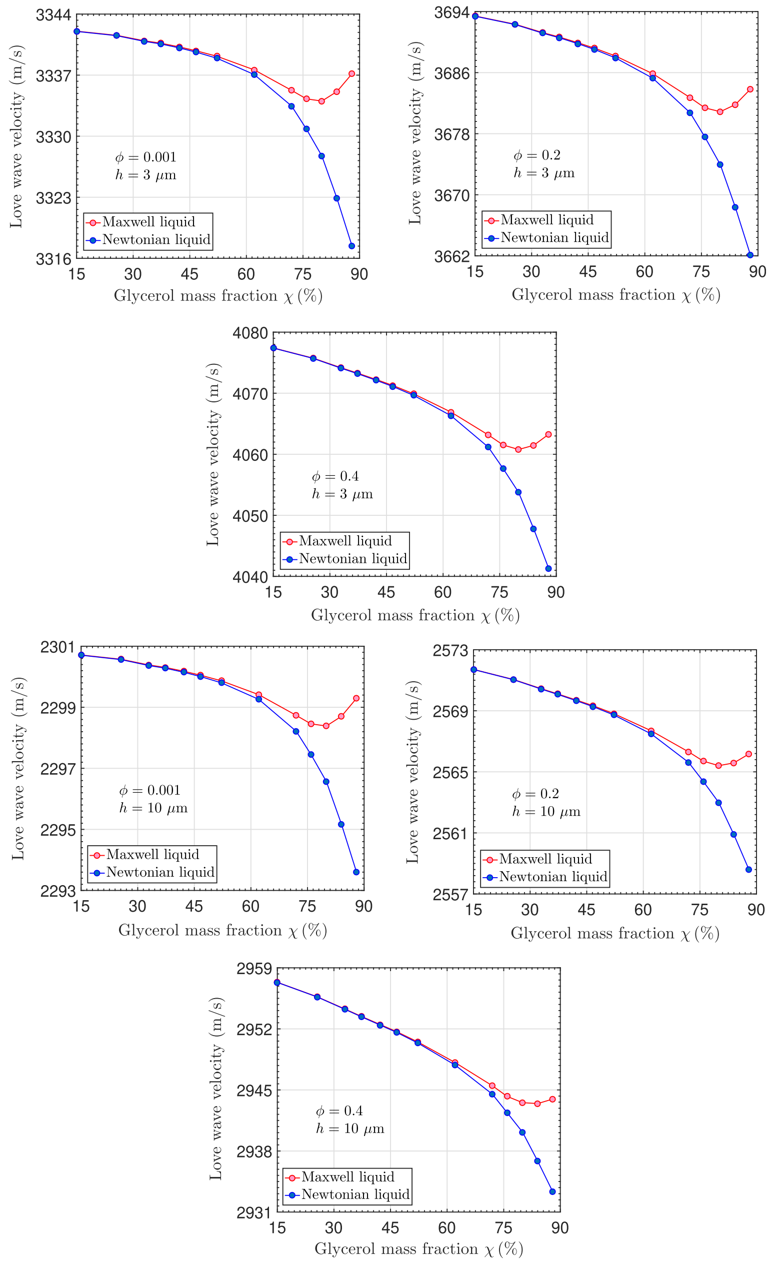

Fig. 6. Velocity for the first mode versus glycerol mass fraction with $f = 100$ MHz.

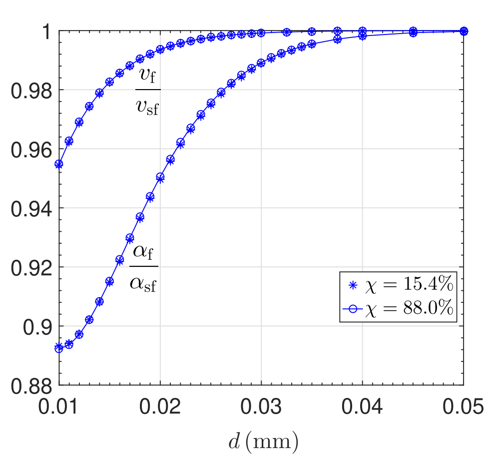

Fig. 7. Normalized velocity and attenuation for the first mode versus substrate thickness d with $\phi = 0.2, h = 3$ μm and $f = 100$ MHz.

and attenuation (α_f/α_{sf}) decrease when the substrate thickness effect becomes significant and approach unity when the substrate thickness effect is negligible with a thickness around 0.04 mm. Consequently, for substrates thickness greater than or equal to 0.04 mm, the substrate can be considered to be a semi-infinite medium and the Eq. (7) can be used.

4. Conclusions

A novel generalized dispersion equation was proposed in this work to design Love wave liquid sensors. It is observed that there is a significant effect of porosity and viscoelasticity simultaneously in the propagation and attenuation of Love waves in a viscoelastic liquid-saturated poroelastic layer. Results also show that for glycerol concentration values less than the critical value (52.2%), the liquid exhibits purely Newtonian behavior and, an increase in the glycerol mass fraction causes a monotonic reduction of the Love wave velocity. However, a Maxwell liquid predicted a non-monotonic variation. The velocity dispersion between Newtonian and Maxwell behaviors becomes less remarkable as the layer thickness and porosity decreases. Thus, we can conclude that the non-monotonic behavior exhibited the intrinsic viscoelastic properties of liquids.

Declaration of Competing Interest

The authors declare that they have no known competing financial interests or personal relationships that could have appeared to influence the work reported in this paper.

References

[1] Kielczynski P, Plowiec R. Determination of the shear impedance of viscoelastic liquids using love and Bleustein-Gulyaev surface waves. J. Acoust. Soc. Am. 1989;86(2):818–27.

[2] Lange K, Rapp BE, Rapp M. Surface acoustic wave biosensors: a review. Anal. Bioanal. Chem. 2008;391(5):1509–19.

[3] Wang W, Oh H, Lee K, Yang S. Enhanced sensitivity of wireless chemical sensor based on love wave mode. Jpn. J. Appl. Phys. 2008;47(9):7372–9.

[4] Oh HK, Wang W, Lee K, Min C, Yang S. The development of a wireless love wave biosensor on 41° YX LiNbO3. Smart Mater. Struct. 2009;18(2).

[5] Rostocki AJ, Siegoczynski RM, Kielczynski P, Szalewski M. An application of love Sh waves for the viscosity measurements of triglycerides at high pressures. High Pressure Res. 2010;30(1):88–92.

[6] Chen X, Liu D. Analysis of viscosity sensitivity for liquid property detection applications based on saw sensors. Mater. Sci. Eng.: C 2010;30(8):1175–82.

[7] Kielczynski P, Szalewski M, Balcerzak A, Rostocki AJ, Tefelski D. Application of Sh surface acoustic waves for measuring the viscosity of liquids in function. Ultrasonics 2011;51(8):921–4.

[8] Liu J. A simple and accurate model for love wave based sensors: dispersion equation and mass sensitivity. AIP Adv. 2014;4(7):1–11.

[9] Kielczynski P, Szalewski M, Balcerzak A. Inverse procedure for simultaneous evaluation of viscosity and density of Newtonian liquids from dispersion curves of Love waves. J. Appl. Phys. 2014;116(4).

[10] Hoang TB, Hanke U, Johannessen EA, Johannessen A. Design of a love wave mode device for use in a microfabricated glucose sensor. IEEE Int. Frequency Control Symposium (IFCS) 2016;1–5.

[11] Caliendo C, Hamidullah M. Guided acoustic wave sensors for liquid environments. J. Phys. D: Appl. Phys. 2019;52.

[12] El Baroudi A, Le Pommellec JY. Viscoelastic fluid effect on the surface wave propagation. Sens. Actuators A: Phys. 2019;291:188–95.

[13] Biot MA. Theory of propagation of elastic waves in a fluid-saturated porous solid-I: low-frequency range. J. Acoust. Soc. Am. 1956;28(2):168–78.

[14] Biot MA. Generalized theory of acoustic propagation in porous dissipative media. J. Acoust. Soc. Am. 1962;34(9):1254–64.

[15] El Baroudi A. Influence of poroelasticity of the surface layer on the surface love wave propagation. J. Appl. Mech. 2018;85.

[16] Joseph DD. Fluid dynamics of viscoelastic liquids. Springer; 1990.